

CONTEXT PARAMETRIZATION WITH COMPOSITIONAL ADAPTERS

Josip Jukić Martin Tutek Jan Šnajder

TakeLab, University of Zagreb

{josip.jukic, martin.tutek, jan.snjader}@fer.hr

ABSTRACT

Large language models (LLMs) often seamlessly adapt to new tasks through in-context learning (ICL) or supervised fine-tuning (SFT). However, both of these approaches face key limitations: ICL is inefficient when handling many demonstrations, and SFT incurs training overhead while sacrificing flexibility. Mapping instructions or demonstrations from context directly into adapter parameters offers an appealing alternative. While prior work explored generating adapters based on a single input context, it has overlooked the need to integrate multiple chunks of information. To address this gap, we introduce COMPAS, a meta-learning framework that translates context into adapter parameters with a compositional structure. Adapters generated this way can be merged algebraically, enabling instructions, demonstrations, or retrieved passages to be seamlessly combined without reprocessing long prompts. Critically, this approach yields three benefits: lower inference cost, robustness to long-context instability, and establishes a principled solution when input exceeds the model’s context window. Furthermore, COMPAS encodes information into adapter parameters in a reversible manner, enabling recovery of input context through a decoder, facilitating safety and security. Empirical results on diverse multiple-choice and extractive question answering tasks show that COMPAS outperforms ICL and prior generator-based methods, especially when scaling to more inputs. Our work establishes composable adapter generation as a practical and efficient alternative for scaling LLM deployment.

1 INTRODUCTION

Large language models (LLMs) adapt to new tasks by integrating *contextual information* pertaining to these tasks, such as instructions, demonstrations, or extracted evidence. This adaptability is typically realized through in-context learning (ICL) (Brown et al., 2020), instruction following (Ouyang et al., 2022), and retrieval-augmented generation (Lewis et al., 2020; Borgeaud et al., 2022), where extra tokens in the prompt act as a transient memory that steers model behavior. Another common strategy is to adapt parameters directly through *supervised fine-tuning* (SFT), ranging from full model updates (Devlin et al., 2019; Raffel et al., 2020) to parameter-efficient variants Pfeiffer et al. (2023). While effective, both prompting and SFT face limitations. Prompt-based methods often require long contexts, which destabilize attention and degrade performance as length increases (Liu et al., 2024), while also incurring inference costs that scale with context size. SFT, on the other hand, requires additional training overhead and lacks flexibility across tasks.

A complementary line of work views *adapters* (Houlsby et al., 2019; Hu et al., 2022) as a mechanism for parametrizing context. In our work, we use *context* as an umbrella term for instructions, demonstrations, or supporting passages. By translating context into parameters, adapters offer a persistent representation that replaces prompt tokens, thereby improving the stability of processing long contexts and amortizing adaptation across tasks (Mahabadi et al., 2021; He et al., 2022; Liu et al., 2024). Once context is encoded into adapters, inference requires only the query tokens, reducing the cost of processing long prompts and making the approach especially attractive in latency- or memory-constrained settings. This context-to-adapter transformation encodes an otherwise transient token sequence into a manipulable object, allowing for caching, reuse, and algebraic combination.

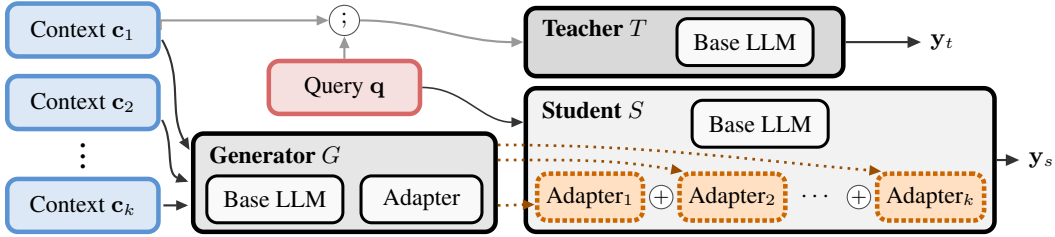


Figure 1: Overview of the COMPAS framework. Each context c_i is mapped into an adapter by the generator G , while the query q is processed by the student S . The teacher T processes the concatenated input $[c; q]$, and G is trained so that composed adapters in S align y_s with y_t .

Building on this perspective, recent work has leveraged meta-learning to efficiently generate adapter parameters directly from support examples without fine-tuning anew for each context (Bansal et al., 2022; Chen et al., 2025). These works largely focused on producing adapters from a single *context*. In practice, however, contexts rarely occur in isolation. Tasks are often guided by chains of instructions, multiple demonstrations, or sets of retrieved passages that must be integrated. Without a principled notion of composition, such adapters cannot faithfully capture how LLMs combine multiple sources of context. Composability also addresses the limitations of prompt-based adaptation. Instead of concatenating long contexts, adapters can be merged algebraically in parameter space. The key challenge is therefore not parameter generation alone, but algebraically consistent composition that preserves semantics of concatenated texts while retaining efficient inference.

To bridge this critical gap, we introduce COMPAS (**Compositional Adapters**), a framework that maps context into adapter parameters with compositional structure at its core. See Figure 1 for a high-level overview. In COMPAS, a teacher LM process concatenates contexts, while the student LM learns to approximate this behavior using only query tokens, complemented with the sum of adapters generated for individual contexts. This is facilitated by a generator network, which maps individual contexts into compositional adapters. COMPAS is driven by auxiliary compositionality and reconstruction losses, which provide diagnostics for whether parameter-space operations preserve semantics and faithfulness (Jacovi & Goldberg, 2020; Turpin et al., 2023; Lampinen et al., 2022). We evaluate COMPAS on multiple-choice and extractive QA tasks, where either demonstrations (MMLU, ARC-Challenge) or retrieved passages (HotpotQA) serve as context. We observe consistent improvements over ICL, fine-tuning and existing context-to-parameter methods. These gains are most pronounced when scaling to larger numbers of demonstrations, highlighting the capacity of COMPAS for efficient integration of external evidence in parameter-space.

Our contributions are threefold: (1) We introduce COMPAS, a teacher-student framework for encoding context into adapters which facilitates composition in parameter space. (2) We establish theoretical conditions under which parameter-space addition provably approximates the behavior of the teacher model. (3) We empirically show that COMPAS outperforms alternatives, especially when scaling to large context sizes, demonstrating the benefits of compositional integration of information.

2 ADAPTER COMPOSITIONALITY

Our goal is to ensure that adapters generated from individual contexts can be *composed* in parameter space to replicate the effect of context concatenation in input space. More concretely, in a teacher-student setup, the outputs of the teacher LM produced when given multiple contexts jointly should be reproduced by the student LM using only the query tokens along with the sum of the corresponding adapter parameters. We now formalize this requirement, introducing conditions under which adapter addition in the parameter space corresponds to context concatenation in the input space.

2.1 SETUP

Let V be the vocabulary and $|V|$ its size. A language model with frozen parameters $\theta \in \mathbb{R}^n$ is a function $f_\theta : \mathcal{X} \rightarrow \mathbb{R}^{|V|}$, where $\mathcal{X} = \Sigma^*$ is the set of all token sequences over the alphabet Σ . For

$\mathbf{x} \in \mathcal{X}$, the output $\mathbf{f}_\theta(\mathbf{x}) \in \mathbb{R}^{|V|}$ denotes the logit vector over the vocabulary. A *support context* $\mathbf{c} \in \mathcal{C}$ is any textual information (e.g., a demonstration, instruction, or retrieved passage) provided alongside a query $\mathbf{q} \in \mathcal{X}$, where $\mathcal{C} \subseteq \mathcal{X}$ denotes the set of admissible contexts. We use $[\mathbf{c}; \mathbf{q}] \in \mathcal{X}$ to denote the concatenation of a context \mathbf{c} with the query \mathbf{q} . Let $\Phi \subseteq \mathbb{R}^m$ denote the set of adapter parameters, and let $\phi \in \Phi$ denote parameters for a single adapter, i.e., a structured modification of θ . We write $\theta \oplus \phi$ for the parameters obtained by composing θ with ϕ .

The **teacher** model corresponds to the base LM applied to the concatenated input: $\mathbf{f}_T(\mathbf{c}, \mathbf{q}) := \mathbf{f}_\theta([\mathbf{c}; \mathbf{q}])$. The **student** model processes only the query, under parameters modified by the adapter: $\mathbf{f}_S^\phi(\mathbf{q}) := \mathbf{f}_{\theta \oplus \phi}(\mathbf{q})$. For a sequence contexts $\mathbf{c}_1, \dots, \mathbf{c}_k$, the teacher takes the concatenation $[\mathbf{c}_1; \dots; \mathbf{c}_k; \mathbf{q}]$, while the student uses the query together with the summed adapter $\sum_{i=1}^k \phi_i$. For example, with two contexts, \mathbf{c}_1 and \mathbf{c}_2 , the student reduces to $\mathbf{f}_S^{\phi_1 + \phi_2}(\mathbf{q}) = \mathbf{f}_{\theta \oplus (\phi_1 + \phi_2)}(\mathbf{q})$. Finally, a **generator** $G : \mathcal{C} \rightarrow \Phi$ maps each context $\mathbf{c} \in \mathcal{C}$ into an adapter $\phi = G(\mathbf{c})$. In particular, for a pair of contexts \mathbf{c}_1 and \mathbf{c}_2 we define $\phi_1 := G(\mathbf{c}_1)$, $\phi_2 := G(\mathbf{c}_2)$, and $\phi_{12} := G([\mathbf{c}_1; \mathbf{c}_2])$.

2.2 COMPOSITIONALITY BOUND

The set of finite contexts \mathcal{C} , equipped with concatenation and the empty string identity (λ), forms a free monoid $(\mathcal{C}, [\cdot; \cdot], \lambda)$. On the other hand, the adapter space $(\Phi, +, \mathbf{0})$ is a commutative additive monoid. A fundamental requirement for adapter compositionality is that the generator $G : \mathcal{C} \rightarrow \Phi$ be a monoid homomorphism, $G([\mathbf{c}_1; \mathbf{c}_2]) = G(\mathbf{c}_1) + G(\mathbf{c}_2)$ and $G(\lambda) = \mathbf{0}$, so that addition in the adapter space exactly mirrors concatenation in the input space. Demanding G to be a homomorphism aligns these two structures. Concatenation on \mathcal{C} is associative but not commutative, whereas addition on Φ is both. Thus, requiring G to be a homomorphism implicitly collapses the order of contexts. This means that G is a non-injective homomorphism: permuted concatenations map to the same adapter sum. We regard this loss of order as desirable in many cases, as the contribution of a demonstration or retrieved passage should often be independent of its relative position. By treating contexts as a set rather than a sequence, we aim for adapters that focus on semantics, mitigating the order sensitivity and instability observed in long-context transformers.¹

Enforcing a homomorphism between the free monoid of contexts and the additive monoid of adapter parameters via a teacher–student setup cannot be achieved exactly in practice, given the models’ finite representational capacity, the finiteness of the training sample, and the approximate nature of optimization. We therefore approximate it, which introduces discrepancies. To capture these discrepancies and regularity conditions, we introduce three quantities.

Student–teacher error. For a context \mathbf{c} with the corresponding adapter $\phi = G(\mathbf{c})$, the student’s discrepancy from the teacher is

$$\epsilon(\mathbf{c}) := \|\mathbf{f}_S^\phi(\mathbf{q}) - \mathbf{f}_T([\mathbf{c}; \mathbf{q}])\|_2, \quad (1)$$

Generator additivity error. The generator’s deviation from additivity is

$$\eta := \|G([\mathbf{c}_1; \mathbf{c}_2]) - (G(\mathbf{c}_1) + G(\mathbf{c}_2))\|_2. \quad (2)$$

Parameter sensitivity. The student’s logits vary smoothly with respect to adapter parameters, with a Lipschitz constant

$$L := \sup_{\phi_1, \phi_2, \mathbf{q}} \frac{\|\mathbf{f}_S^{\phi_1}(\mathbf{q}) - \mathbf{f}_S^{\phi_2}(\mathbf{q})\|_2}{\|\phi_1 - \phi_2\|_2}. \quad (3)$$

The first two quantities capture the core requirements of compositionality, while the third provides a regularity condition needed for the analysis. Assuming $L < \infty$, i.e., Lipschitz continuity of the student with respect to adapter parameters, we obtain the following result.

Theorem 1 (Compositionality Bound). *For any contexts $\mathbf{c}_1, \mathbf{c}_2$, and query \mathbf{q} , with $\phi_i = G(\mathbf{c}_i)$,*

$$\|\mathbf{f}_S^{\phi_1 + \phi_2}(\mathbf{q}) - \mathbf{f}_T([\mathbf{c}_1; \mathbf{c}_2; \mathbf{q}])\|_2 \leq L\eta + \epsilon([\mathbf{c}_1; \mathbf{c}_2]).$$

¹Certain tasks may still require positional information (e.g., reasoning with ordered evidence). We show in Appendix C.3 that our framework can incorporate explicit positional encodings when needed.

See Section A for the proof. The bound decomposes the student–teacher error into two interpretable sources: generator additivity error (η) and misfit on the concatenated context ($\epsilon([\mathbf{c}_1; \mathbf{c}_2])$). The Lipschitz constant L propagates generator errors into the student. Thus, perfect compositionality is unattainable in practice, but approximate compositionality is achievable whenever these quantities remain small.

3 METHOD

Previously, we decomposed the discrepancy between *context concatenation* and *adapter addition* into two main error sources: generator additivity error (η) and student–teacher error on concatenated contexts (ϵ), with parameter sensitivity (L) controlling how generator errors propagate to outputs. While L is a structural property of the student model, we can *design* the generator and its training objectives to directly minimize η and ϵ . To this end, we introduce COMPAS, a teacher–student meta-learning framework that maps each support context into a LoRA adapter (Hu et al., 2022), which is composed additively with the base parameters. The adapter generator ends with a linear bottleneck, ensuring that its outputs in parameter space add directly. This algebraic addition is trained to approximate the *outputs* of the model under context concatenation in input space. To achieve this, we design loss functions that incentivize the generator to approximate a homomorphism from context concatenation to parameter-space addition.

3.1 CONTEXT-TO-ADAPTER GENERATOR

As introduced in Section 2, the generator G maps a context \mathbf{c} to adapter parameters $\phi = G(\mathbf{c})$. It is implemented by augmenting the base LM with additional trainable components: (i) its own LoRA adapter inserted into the LM, and (ii) a linear bottleneck followed by two projection trunks. The same frozen base LM is shared across the teacher, the student, and the generator, where only the generator’s adapter and projection components are updated during training.

Given a support context \mathbf{c} , the base LM (with the generator’s adapter) processes the tokens, and we obtain $\mathbf{h}(\mathbf{c}) \in \mathbb{R}^d$ as the mean of the final-layer hidden states across all tokens. This pooled representation is projected into a compact latent space,

$$\mathbf{z}(\mathbf{c}) = P \mathbf{h}(\mathbf{c}), \quad P \in \mathbb{R}^{r \times d}, \quad r \ll d,$$

reducing dimensionality and ensuring the subsequent mapping into LoRA parameters remains tractable. Without this bottleneck, a direct mapping would require prohibitively many parameters.

A LoRA module applied to a target linear map with input dimension d^{in} and output dimension d^{out} consists of two low-rank matrices $\mathbf{A} \in \mathbb{R}^{r \times d^{\text{in}}}$ and $\mathbf{B} \in \mathbb{R}^{d^{\text{out}} \times r}$, with rank $r \ll d^{\text{in}}, d^{\text{out}}$. Each transformer layer may contain multiple such modules (e.g., query, key, value, or output projections). Let \mathcal{M} denote the set of all modules instrumented with LoRA, indexed across layers and projection types. From the latent representation $\mathbf{z}(\mathbf{c})$, the generator produces parameters for all modules via two bias-free linear projections: $U_A \mathbf{z}(\mathbf{c}) \in \mathbb{R}^{m_A}$ and $U_B \mathbf{z}(\mathbf{c}) \in \mathbb{R}^{m_B}$, with

$$m_A = \sum_{m \in \mathcal{M}} r_m d_m^{\text{in}}, \quad m_B = \sum_{m \in \mathcal{M}} d_m^{\text{out}} r_m.$$

The outputs of U_A and U_B are partitioned and reshaped into the individual LoRA matrices $\mathbf{A}_m(\mathbf{c})$ and $\mathbf{B}_m(\mathbf{c})$ for each target module $m \in \mathcal{M}$. See Figure 1 for a high-level overview of COMPAS.

3.2 LOSS FUNCTION COMPONENTS

Our loss function design follows Theorem 1: we reduce the student–teacher error in both single and concatenated contexts, and penalize generator non-additivity. We also include a reconstruction term that encourages adapters to faithfully encode their contexts (up to permutation), preventing collapse into trivial solutions. This auxiliary objective also regularizes training and provides a stronger learning signal, aiding optimization.

Student–teacher alignment. We draw unlabeled queries \mathbf{q} and contexts of length $k \in \{1, 2\}$, letting the teacher provide soft pseudo-labels (logits). The student is trained to match these through

weak supervision:

$$\mathcal{L}_{\text{ST}} = \mathbb{E}_{((\mathbf{c}_1, \dots, \mathbf{c}_k), \mathbf{q})} \left[\text{KL} \left(\text{softmax}(\mathbf{f}_T([\mathbf{c}_1; \dots; \mathbf{c}_k; \mathbf{q}])) \parallel \text{softmax}(\mathbf{f}_S^{\sum_{i=1}^k \phi_i}(\mathbf{q})) \right) \right].$$

where KL denotes Kullback–Leibler divergence. For $k = 1$ this enforces single-context fidelity, while for $k = 2$ it enforces compositionality.

Additivity regularization. We reduce the generator additivity error η by penalizing discrepancies between parameters generated for concatenated contexts and the sum of parameters from the individual contexts. Concretely, we draw pairs of contexts $(\mathbf{c}_1, \mathbf{c}_2)$ and compare generated parameters:

$$\mathcal{L}_{\text{ADD}} = \mathbb{E}_{(\mathbf{c}_1, \mathbf{c}_2)} \left[\sum_{m \in \mathcal{M}} \frac{\|\mathbf{W}_m([\mathbf{c}_1; \mathbf{c}_2]) - (\mathbf{W}_m(\mathbf{c}_1) + \mathbf{W}_m(\mathbf{c}_2))\|_F^2}{\|\mathbf{W}_m([\mathbf{c}_1; \mathbf{c}_2])\|_F^2 + \delta} \right],$$

where $\mathbf{W}_m(\mathbf{c}) \in \{\mathbf{A}_m(\mathbf{c}), \mathbf{B}_m(\mathbf{c})\}$ denotes either of the two LoRA matrices generated for module $m \in \mathcal{M}$, $\|\cdot\|_F$ is the Frobenius norm, and $\delta > 0$ is a small constant for stability.

Reconstruction. To encourage faithfulness and improve training stability, we require adapters to recoverably encode the information contained in their contexts. We introduce a special query token `[RECON]`, which prompts the student to reconstruct the support context from its adapter in an autoregressive manner. This discourages collapse to trivial solutions and provides an auxiliary learning signal through the cross-entropy (CE) loss:

$$\mathcal{L}_{\text{RECON}} = \mathbb{E}_{\mathbf{c}} \left[\text{CE}(\mathbf{c}, \mathbf{f}_S^\phi([\text{RECON}])) \right].$$

Overall objective. The final loss function is a weighted sum:

$$\mathcal{L}_{\text{COMPAS}} = \lambda_{\text{ST}} \mathcal{L}_{\text{ST}} + \lambda_{\text{ADD}} \mathcal{L}_{\text{ADD}} + \lambda_{\text{RECON}} \mathcal{L}_{\text{RECON}}. \quad (4)$$

Hyperparameter choices and training details are provided in Section B.

4 EXPERIMENTS

We first outline the experimental design §4.1, with full setup and hyperparameter details in Section B. We then evaluate COMPAS in two regimes: (i) replacing in-context demonstrations with adapter parameters (§4.2), and (ii) encoding retrieved passages as parametric memory (§4.3). Finally, we assess reconstruction, measuring faithfulness of information encoded in adapter parameters (§4.4). Additional experiments on context order sensitivity and efficiency are in Section C.

4.1 EXPERIMENTAL SETUP

Models. We experiment with decoder-only LMs: **LLaMA-3.1 8B** (LLaMA 8B) and **Llama-3.2 3B** (Grattafiori et al., 2024), and **Qwen-2.5 7B** (Yang et al., 2025). For brevity, we refer to these models as LLaMA 8B, LLaMA 3B, and Qwen 7B.

Tasks. We consider two representative settings: (i) ICL on **MMLU** (Hendrycks et al., 2021) and **ARC-Challenge** (Clark et al., 2018), where few-shot exemplars are provided as demonstrations; (ii) Extractive question answering (QA) on **HotpotQA** (Yang et al., 2018), where gold passages supply contextual evidence. Prompts and preprocessing are standardized across all methods (Section D).

Methods. We compare against three representative approaches. **ICL** is standard k -shot prompting with demonstrations concatenated in prompt text. **Generative Adapter (GenAda)** (Chen et al., 2025) employs a nonlinear hypernetwork to predict adapter weights from context, trained with reconstruction and continuation losses. In contrast, our method enforces a linear bottleneck, generating adapters via a lightweight adapter module followed by a linear transformation. **WILDA** (Jukić & Šnajder, 2025) fine-tunes a separate adapter for each context, achieving strong accuracy but incurring heavy computational overhead, since a new adapter must be trained for every context.

Table 1: Demonstration parameterization results. Rows with a single number indicate concatenation of all demonstrations without composition, while rows of the form $a \times b$ denote composition of a adapters, each encoding b demonstrations. Results are reported as the mean over 10 runs with the standard deviation as a subscript. The best score within each block is highlighted in **bold**. COMPAS results are statistically compared to the corresponding ICL setting; scores marked with \dagger indicate significance under a Wilcoxon signed-rank test ($p < 0.05$) with Holm–Bonferroni correction.

Setup / Method	Llama-3.1 8B		Llama-3.2 3B		Qwen-2.5 7B	
	MMLU	ARC	MMLU	ARC	MMLU	ARC
4 ICL	64.2 _{1.8}	74.2 _{1.6}	57.2 _{1.8}	62.9 _{1.6}	70.2 _{1.8}	76.5 _{1.6}
4 GenAda	57.6 _{1.8}	69.3 _{1.7}	50.4 _{1.4}	59.4 _{1.7}	59.8 _{2.1}	70.5 _{1.7}
4 WILDA	68.8 _{0.9}	78.2 _{0.7}	60.8 _{1.1}	66.4 _{1.2}	74.0 _{0.4}	79.6 _{0.9}
4 COMPAS	66.7 _{0.7} [†]	76.5 _{0.8} [†]	59.0 _{0.9}	65.1 _{0.8} [†]	72.4 _{0.5} [†]	77.2 _{0.6}
8 ICL	65.5 _{1.7}	75.1 _{1.5}	58.0 _{1.7}	64.1 _{1.5}	71.5 _{1.7}	78.3 _{1.5}
8 GenAda	59.1 _{1.9}	69.9 _{1.6}	51.3 _{1.9}	61.2 _{1.6}	60.7 _{1.9}	71.4 _{1.6}
8 WILDA	69.8 _{0.7}	78.8 _{0.8}	61.2 _{1.1}	67.4 _{0.5}	74.8 _{0.7}	80.0 _{0.8}
8 COMPAS	67.5 _{0.5}	77.2 _{0.9} [†]	60.2 _{1.3} [†]	66.2 _{0.5} [†]	73.2 _{1.2}	78.6 _{0.7}
2×4 GenAda	57.8 _{1.9}	69.5 _{1.6}	50.9 _{0.7}	59.4 _{1.2}	60.5 _{1.8}	69.2 _{1.6}
2×4 WILDA	69.5 _{0.3}	78.6 _{0.9}	60.8 _{1.1}	67.1 _{1.0}	74.1 _{0.4}	79.8 _{0.8}
2×4 COMPAS	69.1 _{0.7} [†]	79.3 _{0.9} [†]	61.3 _{1.2} [†]	66.8 _{0.6} [†]	74.6 _{0.6} [†]	80.2 _{0.9}
12 ICL	66.0 _{1.7}	75.5 _{1.5}	58.8 _{1.7}	64.6 _{1.5}	71.8 _{1.7}	77.2 _{1.5}
12 GenAda	59.9 _{1.9}	70.2 _{1.6}	51.6 _{1.9}	62.5 _{1.6}	63.1 _{1.9}	71.6 _{1.2}
12 WILDA	70.5 _{0.8}	79.4 _{0.6}	61.9 _{1.1}	68.1 _{1.0}	75.2 _{0.7}	79.8 _{0.4}
12 COMPAS	67.2 _{1.2}	78.9 _{0.9} [†]	59.5 _{1.2}	67.2 _{0.7} [†]	72.9 _{1.0}	79.3 _{1.4}
3×4 GenAda	57.3 _{1.9}	70.3 _{1.6}	49.8 _{1.9}	59.6 _{1.6}	62.0 _{1.9}	69.7 _{1.6}
3×4 WILDA	70.7 _{1.0}	79.5 _{0.9}	62.0 _{1.1}	67.5 _{1.0}	75.1 _{0.7}	79.9 _{0.4}
3×4 COMPAS	71.2 _{1.1} [†]	80.1 _{0.5} [†]	62.4 _{0.8} [†]	67.4 _{0.9}	75.7 _{0.3} [†]	80.3 _{0.8} [†]
16 ICL	66.5 _{1.7}	76.0 _{1.5}	59.2 _{1.7}	65.2 _{1.5}	72.3 _{1.7}	77.6 _{1.5}
16 GenAda	60.5 _{1.9}	72.5 _{1.6}	52.7 _{1.2}	60.8 _{1.3}	64.2 _{1.4}	71.9 _{0.9}
16 WILDA	71.5 _{0.7}	80.4 _{0.3}	62.6 _{0.5}	68.2 _{0.3}	76.1 _{0.4}	80.7 _{0.8}
16 COMPAS	68.2 _{0.6}	79.1 _{0.7} [†]	62.3 _{1.2}	68.3 _{0.4} [†]	73.7 _{0.6}	79.4 _{0.5}
4×4 GenAda	57.6 _{1.9}	70.6 _{1.6}	50.3 _{1.9}	59.9 _{1.6}	61.3 _{1.9}	70.4 _{1.6}
4×4 WILDA	71.6 _{0.6}	80.5 _{0.9}	62.7 _{1.1}	68.3 _{1.1}	75.2 _{0.5}	80.8 _{0.8}
4×4 COMPAS	72.2 _{0.3} [†]	81.3 _{0.3} [†]	63.4 _{0.7} [†]	69.3 _{0.5} [†]	77.1 _{0.7} [†]	81.5 _{0.4} [†]

Evaluation. We assess models on end-task performance, measuring accuracy on MMLU and ARC and exact match (EM) and token-level F1 on HotpotQA. Faithfulness is evaluated through the KL divergence between the teacher concatenation and the student sum, as well as token-level F1 (*bag-of-tokens*). Stability is measured as the standard deviation across ten runs with different sampled contexts. Training follows the weakly supervised protocol from §3.2. Full implementation details, including optimization settings and hyperparameters, are deferred to Section B.

4.2 ENCODING DEMONSTRATIONS AS PARAMETERS

We first evaluate COMPAS effectiveness in replacing in-context demonstrations with adapter parameters. In the k -shot setting ($k \in \{4, 8, 12, 16\}$), demonstrations are partitioned into fixed-size blocks, each block is encoded as an adapter, and the adapters are composed by summing their parameters. Table 1 shows the results on MMLU and ARC-Challenge across three base models.

COMPAS *consistently outperforms standard ICL*, which in our setup corresponds to using the teacher model directly, across all models and shot counts, while also exhibiting lower variance. We attribute this robustness to weak-to-strong (W2S) generalization (Dherin et al., 2022; Lang et al., 2024): the student begins with weak pseudo-labels from the teacher but progressively corrects them during training, extending reliability from easy, locally consistent regions to harder examples.

Gains are most pronounced at higher shot counts ($k \in 12, 16$) under 3×4 and 4×4 composition settings, where COMPAS consistently outperforms WILDA (11 out of 12 cases), despite the latter’s

Table 2: Extractive QA results on single, pair, and triplet gold contexts, averaged over 10 runs and reported as EM/F1. *Teacher (concat)* evaluates the base LLM directly on concatenated gold contexts (e.g., $[c_1; c_2; c_3]$). COMPAS (*concat*) evaluates the student using an adapter generated from the concatenated context, $G([c_1; c_2; c_3])$, while COMPAS (*composed*) uses the sum of adapters from individual contexts, $\sum_i G(c_i)$.

Setup	Method	LLaMA-3.1 8B	LLaMA-3.2 3B	Qwen-2.5 7B
Single (c)	Teacher	70.9/82.0	65.9/78.1	69.2/80.7
	COMPAS	72.2/82.9	67.0/78.6	69.4/82.2
Pair ($[c_1; c_2]$)	Teacher (concat)	69.0/80.8	64.1/76.8	67.5/79.8
	COMPAS (concat)	69.4/81.1	64.5/77.0	67.9/79.5
	COMPAS (composed)	71.3/82.3	66.2/78.4	69.6/80.9
Triplet ($[c_1; c_2; c_3]$)	Teacher (concat)	66.3/78.5	61.2/74.1	64.0/76.0
	COMPAS (concat)	67.5/79.4	62.0/75.3	65.1/77.0
	COMPAS (composed)	71.1/82.0	64.8/76.9	68.1/80.4

Table 3: COMPAS context reconstruction as token-level F1. Results are averages over 10 runs. MMLU and ARC *units* are blocks of 4 demonstrations; a HotpotQA *unit* is a supporting paragraph.

Setup	Llama-3.1 8B			Llama-3.2 3B			Qwen-2.5 7B		
	MMLU	ARC	Hotpot	MMLU	ARC	Hotpot	MMLU	ARC	Hotpot
Single (1 unit)	91.2	89.5	87.8	89.0	87.2	85.4	90.1	88.1	86.2
Pair (2 units)	90.3	88.9	86.0	88.1	86.3	83.5	89.4	87.5	84.3
Triplet (3 units)	88.4	86.9	83.7	86.5	84.8	81.9	87.6	85.9	82.5

use of context-specific adapter fine-tuning. We hypothesize that this advantage arises from an implicit chunking-composition mechanism, where the model partitions demonstrations into manageable subsets. Each adapter encodes a partial context view, and their addition reconstructs the effect of all demonstrations. As a result, COMPAS scales gracefully with the number of demonstrations: it leverages composition to maintain strong performance in long contexts, ultimately matching or exceeding specialized adapter fine-tuning while retaining efficiency and composability.

4.3 ENCODING CONTEXT AS PARAMETRIC MEMORY

We now evaluate COMPAS on extractive QA by treating gold evidence passages as *parametric memories*. On HotpotQA, each query q is paired with one or more gold passages c . When multiple passages are available (pairs or triplets), the task becomes more challenging: the model must leverage a larger combined context and answer more queries. In these settings, we either generate a single adapter from their concatenation or compose the adapters generated from each passage individually. We evaluate per query, including all gold passages in either form. Results are shown in Table 2.

COMPAS consistently outperforms the teacher (base LLM) across all settings. Absolute performance is lower on pairs and triplets – since the model must retain context for multiple queries while being evaluated on each one separately – but the relative gains over the teacher are larger in these harder settings. This indicates that COMPAS is particularly effective at composing and retaining information across multiple contexts.

4.4 CONTEXT RECONSTRUCTION

Finally, we test whether composed adapters preserve the informational content of their supports by prompting the model to reconstruct missing contexts. Using a special [RECON] token, we decode from adapters and compute token-level F1 on MMLU, ARC, and HotpotQA. Table 3 shows that COMPAS maintains consistently high reconstruction fidelity, with only small drops as the context expands to pair and triplet units.

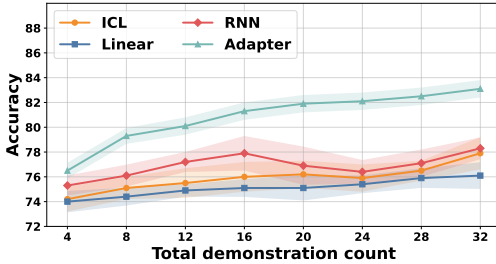


Figure 2: Effect of generator capacity on accuracy with LLaMA 8B on ARC-Challenge. Shaded areas show deviation over 10 runs.

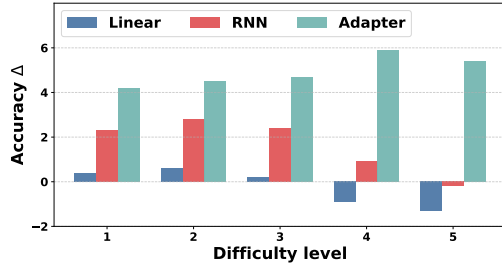


Figure 3: Accuracy deltas of different generators over ICL across five MMLU difficulty buckets (average over 10 runs for LLaMA 8B).

5 ANALYSIS

Building on the effectiveness of COMPAS, we analyze the role of generator capacity (§5.1) and the contribution of each loss component (§5.2). We discuss limitations of our approach in Section E.

5.1 CAPACITY AND WEAK-TO-STRONG GENERALIZATION

We explore three generator capacities G : **Adapter** (COMPAS) – corresponds to our default setup (§3); **RNN** – a lightweight recurrent network which aggregates token-level encodings of c before the same linear head produces $G(c)$; **Linear** – an ablation that removes the generator adapter and recurrent aggregator, leaving a single bottleneck linear projection of a pooled context representation (see configuration details in Section B).

In Figure 2, we compare the performance of generators with varying capacity as the number of demonstrations increases. A simple linear generator initially tracks the performance of the ICL teacher, but falls behind as more demonstrations are added, indicating limited ability to capture multi-shot composition. The *RNN* generator improves on ICL and linear baselines for moderate demonstration counts, but eventually stagnates. In contrast, the *Adapter* generator consistently outperforms alternatives, and its advantage widens with larger demonstration counts. These results highlight the importance of generator capacity for both surpassing the ICL teacher and maintaining compositionality as context scales.

In Figure 3, we analyze the effects of W2S generalization by grouping MMLU tasks into five difficulty levels (1–5). To obtain these groups, we evaluate the base LLaMA 8B with 16 shots on each MMLU subtask and sort them by accuracy, partitioning into five bins. We then evaluate generators in a 4×4 setup (16 demonstrations in total). Across levels 1–3, all generator variants improve over ICL, with gains ordered by capacity (*Adapter*, *RNN*, and *Linear*). At higher difficulty, differences sharpen: the linear generator collapses at level 4–5, *RNN* stagnates and drops at level 5, while *Adapter* continues to improve, achieving the largest gains on the hardest tasks. These results show that sufficient generator capacity is crucial for surpassing the ICL teacher and maintaining additive composition as complexity grows. COMPAS scales with task difficulty, enhancing W2S generalization on the hardest tasks.

5.2 IMPORTANCE OF LOSS COMPONENTS

To better understand the contribution of each training signal, we perform an ablation study on the loss components of COMPAS. Table 4 reports results on MMLU, ARC-Challenge, and HotpotQA using the LLaMA 8B backbone. We compare the full objective (4) to variants with removed components, isolating their effect on overall performance.

We always include \mathcal{L}_{ST} , since weak supervision from the teacher is essential for transferring contextual information into the student. Dropping \mathcal{L}_{ADD} or \mathcal{L}_{RECON} degrades performance and shows that they play complementary roles. \mathcal{L}_{ADD} reduces additivity error (η) and stabilizes multi-context composition. \mathcal{L}_{RECON} provides smaller but consistent gains while also enabling context reconstruction. Removing both terms (\mathcal{L}_{ADD} and \mathcal{L}_{RECON}) leads to the most pronounced drop, confirming that

Table 4: Ablation of loss function components. Results are on MMLU and ARC (4×4 demos) and HotpotQA (EM/F1, pairs). We report averages over 10 seeds with standard deviations as subscripts.

Objective Variant	MMLU	ARC-Challenge	HotpotQA (EM/F1)
Full	69.1	79.3	71.3/82.3
$-\mathcal{L}_{\text{ADD}}$	64.8	75.7	68.2/79.3
$-\mathcal{L}_{\text{RECON}}$	66.4	77.1	70.2/80.8
\mathcal{L}_{ST} only	61.2	71.8	65.9/76.4

they jointly support the effectiveness of the student. Overall, the full objective yields the strongest results, consistent with the theory in §2.

6 RELATED WORK

ICL and parameterized adaptation. Analyses show ICL often exploits surface-level cues rather than learning task semantics (Min et al., 2022), and that transformers can internally implement simple learning algorithms during inference (Xie et al., 2022; Akyürek et al., 2023). In parallel, *parameter-efficient fine-tuning* (PEFT) replaces long prompts with compact trainable modules such as soft/prefix prompts (Li & Liang, 2021; Lester et al., 2021) or low-rank adapters (Hu et al., 2022). Recently, Hong et al. (2025) proposed mixtures of in-context learners to efficiently combine subsets of demonstrations. Like PEFT, our work keeps inference on the query only, but instead of concatenating demonstrations, we translate them into compositional adapters.

Composing and merging parameters. Another line of research explores how to *compose* learned modules or entire models. In the adapter setting, AdapterFusion learns to fuse multiple task adapters non-destructively (Pfeiffer et al., 2021), while MAD-X composes language and task adapters for cross-lingual transfer (Pfeiffer et al., 2020). For full model weights, *model soups* average fine-tuned checkpoints to improve robustness (Wortsman et al., 2022), and *task vectors* use weight differences to add or subtract task behaviors (Ilharco et al., 2023). These approaches combine pre-trained modules or models after the fact. In contrast, we generate adapters *on-the-fly* from context and train them explicitly for additivity, so that parameter-space composition mirrors text concatenation.

Generating parameters from context. *HyperNetworks* generate parameters of one network using another (Ha et al., 2017). Ansell et al. (2021) introduced MAD-G, where a hypernetwork generates language adapters conditioned on language embeddings. Subsequent work extended this idea to few-shot adaptation (Chen et al., 2025). Our method can be viewed as a hypernetwork explicitly designed for *compositionality*: a generator maps support encodings into LoRA parameters, while compositional distillation and a linearity regularizer enforce that adapter addition in parameter space approximates context concatenation in input space. This aligns with broader efforts to impose linear additive structure on representations, but uniquely emphasizes parameter-space composition as a scalable route to context integration.

7 CONCLUSION

We tackled the challenges of efficiency and instability that arise when adapting LLMs to tasks requiring multiple demonstrations or retrieved passages. To address these issues, we introduced COMPAS, a meta-learning teacher–student framework that translates contexts into *compositional adapters*. COMPAS encodes context into adapter parameters that can be algebraically combined, allowing processing of complex queries without input concatenation. In this way, we enable efficient handling of large context sets by generating adapters independently and composing them in parameter space, reducing inference cost, mitigating long-context degradation, and circumventing context window limitations. A reconstruction objective promotes safety and security, ensuring that the input context is decodable from the adapter parameters. COMPAS consistently outperforms ICL and prior generator-based approaches on multi-choice and extractive question answering. Taken together, these results establish composable context parametrization as a scalable approach for adapting LLMs.

REPRODUCIBILITY STATEMENT

Along with the description of our method in Section 3 and the experimental setup in Section B, we also provide comprehensive details to ensure reproducibility. All datasets used (MMLU, ARC-Challenge, HotpotQA) are publicly available and described in Section 4.1. Model configurations, optimization settings, and training schedules are fully specified in Section B, along with the specified computing infrastructure. Theoretical results, including the proof of Theorem 1 and its corollary, are presented in Section A. Prompt templates for all benchmarks are provided in Section D. In addition, we include code in the supplementary material and will publish the repository publicly after the review process. Collectively, these resources allow independent reproduction and verification of our experiments and analyses.

REFERENCES

Ekin Akyürek, Dale Schuurmans, Jacob Andreas, Tengyu Ma, and Denny Zhou. What learning algorithm is in-context learning? investigations with linear models. In *The Eleventh International Conference on Learning Representations*, 2023. URL <https://openreview.net/forum?id=0g0X4H8yN4I>.

Alan Ansell, Edoardo Maria Ponti, Jonas Pfeiffer, Sebastian Ruder, Goran Glavaš, Ivan Vulić, and Anna Korhonen. Mad-g: Multilingual adapter generation for efficient cross-lingual transfer. In *Findings of EMNLP*, 2021. URL <https://aclanthology.org/2021.findings-emnlp.410/>.

Trapit Bansal, Salaheddin Alzubi, Tong Wang, Jay-Yoon Lee, and Andrew McCallum. Meta-adapters: Parameter efficient few-shot fine-tuning through meta-learning. In *First Conference on Automated Machine Learning (Main Track)*, 2022. URL <https://openreview.net/forum?id=BCGNf-prLg5>.

Sebastian Borgeaud, Arthur Mensch, Jordan Hoffmann, Trevor Cai, Eliza Rutherford, Katie Millican, George Bm Van Den Driessche, Jean-Baptiste Lespiau, Bogdan Damoc, Aidan Clark, Diego De Las Casas, Aurelia Guy, Jacob Menick, Roman Ring, Tom Hennigan, Saffron Huang, Loren Maggiore, Chris Jones, Albin Cassirer, Andy Brock, Michela Paganini, Geoffrey Irving, Oriol Vinyals, Simon Osindero, Karen Simonyan, Jack Rae, Erich Elsen, and Laurent Sifre. Improving language models by retrieving from trillions of tokens. In Kamalika Chaudhuri, Stefanie Jegelka, Le Song, Csaba Szepesvari, Gang Niu, and Sivan Sabato (eds.), *Proceedings of the 39th International Conference on Machine Learning*, volume 162 of *Proceedings of Machine Learning Research*, pp. 2206–2240. PMLR, 17–23 Jul 2022. URL <https://proceedings.mlr.press/v162/borgeaud22a.html>.

Tom Brown, Benjamin Mann, Nick Ryder, Melanie Subbiah, Jared D Kaplan, Prafulla Dhariwal, Arvind Neelakantan, Pranav Shyam, Girish Sastry, Amanda Askell, Sandhini Agarwal, Ariel Herbert-Voss, Gretchen Krueger, Tom Henighan, Rewon Child, Aditya Ramesh, Daniel Ziegler, Jeffrey Wu, Clemens Winter, Chris Hesse, Mark Chen, Eric Sigler, Mateusz Litwin, Scott Gray, Benjamin Chess, Jack Clark, Christopher Berner, Sam McCandlish, Alec Radford, Ilya Sutskever, and Dario Amodei. Language models are few-shot learners. In H. Larochelle, M. Ranzato, R. Hadsell, M.F. Balcan, and H. Lin (eds.), *Advances in Neural Information Processing Systems*, volume 33, pp. 1877–1901. Curran Associates, Inc., 2020. URL https://proceedings.neurips.cc/paper_files/paper/2020/file/1457c0d6bfc4967418bfb8ac142f64a-Paper.pdf.

Tong Chen, Hao Fang, Patrick Xia, Xiaodong Liu, Benjamin Van Durme, Luke Zettlemoyer, Jianfeng Gao, and Hao Cheng. Generative adapter: Contextualizing language models in parameters with a single forward pass. In *International Conference on Learning Representations (ICLR)*, 2025. URL <https://openreview.net/forum?id=bc3sUss6ck>.

Kyunghyun Cho, Bart van Merriënboer, Caglar Gulcehre, Dzmitry Bahdanau, Fethi Bougares, Holger Schwenk, and Yoshua Bengio. Learning phrase representations using RNN encoder–decoder for statistical machine translation. In *Proceedings of the 2014 Conference on Empirical*

Methods in Natural Language Processing (EMNLP), pp. 1724–1734. Association for Computational Linguistics, 2014. doi: 10.3115/v1/D14-1179. URL <https://aclanthology.org/D14-1179>.

Peter Clark, Isaac Cowhey, Oren Etzioni, Tushar Khot, Ashish Sabharwal, Carissa Schoenick, and Oyvind Tafjord. Think you have solved question answering? Try ARC, the AI2 reasoning challenge. *arXiv:1803.05457*, 2018.

Jacob Devlin, Ming-Wei Chang, Kenton Lee, and Kristina Toutanova. BERT: Pre-training of deep bidirectional transformers for language understanding. In Jill Burstein, Christy Doran, and Thamar Solorio (eds.), *Proceedings of the 2019 Conference of the North American Chapter of the Association for Computational Linguistics: Human Language Technologies, Volume 1 (Long and Short Papers)*, pp. 4171–4186, Minneapolis, Minnesota, June 2019. Association for Computational Linguistics. doi: 10.18653/v1/N19-1423. URL <https://aclanthology.org/N19-1423>.

Benoit Dherin, Michael Munn, Mihaela Rosca, and David GT Barrett. Why neural networks find simple solutions: The many regularizers of geometric complexity. In Alice H. Oh, Alekh Agarwal, Danielle Belgrave, and Kyunghyun Cho (eds.), *Advances in Neural Information Processing Systems*, 2022. URL <https://openreview.net/forum?id=-ZPeUAJlkEu>.

Aaron Grattafiori, Abhimanyu Dubey, Abhinav Jauhri, Abhinav Pandey, Abhishek Kadian, Ahmad Al-Dahle, Aiesha Letman, Akhil Mathur, Alan Schelten, Alex Vaughan, Amy Yang, Angela Fan, Anirudh Goyal, Anthony Hartshorn, Aobo Yang, Archi Mitra, Archie Sravankumar, Artem Korenев, Arthur Hinsvark, Arun Rao, Aston Zhang, Aurelien Rodriguez, Austen Gregerson, Ava Spataru, Baptiste Roziere, Bethany Biron, Binh Tang, Bobbie Chern, Charlotte Caucheteux, Chaya Nayak, Chloe Bi, Chris Marra, Chris McConnell, Christian Keller, Christophe Touret, Chunyang Wu, Corinne Wong, Cristian Canton Ferrer, Cyrus Nikolaidis, Damien Allonsius, Daniel Song, Danielle Pintz, Danny Livshits, Danny Wyatt, David Esiobu, Dhruv Choudhary, Dhruv Mahajan, Diego Garcia-Olano, Diego Perino, Dieuwke Hupkes, Egor Lakomkin, Ehab AlBadawy, Elina Lobanova, Emily Dinan, Eric Michael Smith, Filip Radenovic, Francisco Guzmán, Frank Zhang, Gabriel Synnaeve, Gabrielle Lee, Georgia Lewis Anderson, Govind That-tai, Graeme Nail, Gregoire Mialon, Guan Pang, Guillem Cucurell, Hailey Nguyen, Hannah Korevaar, Hu Xu, Hugo Touvron, Iliyan Zarov, Imanol Arrieta Ibarra, Isabel Kloumann, Ishan Misra, Ivan Evtimov, Jack Zhang, Jade Copet, Jaewon Lee, Jan Geffert, Jana Vranes, Jason Park, Jay Mähadeokar, Jeet Shah, Jelmer van der Linde, Jennifer Billcock, Jenny Hong, Jenya Lee, Jeremy Fu, Jianfeng Chi, Jianyu Huang, Jiawen Liu, Jie Wang, Jiecao Yu, Joanna Bitton, Joe Spisak, Jong-soo Park, Joseph Rocca, Joshua Johnstun, Joshua Saxe, Junteng Jia, Kalyan Vasuden Alwala, Karthik Prasad, Kartikeya Upasani, Kate Plawiak, Ke Li, Kenneth Heafield, Kevin Stone, Khalid El-Arini, Kritthika Iyer, Kshitiz Malik, Kuenley Chiu, Kunal Bhalla, Kushal Lakhota, Lauren Rantala-Yearly, Laurens van der Maaten, Lawrence Chen, Liang Tan, Liz Jenkins, Louis Martin, Lovish Madaan, Lubo Malo, Lukas Blecher, Lukas Landzaat, Luke de Oliveira, Madeline Muzzi, Mahesh Pasupuleti, Mannat Singh, Manohar Paluri, Marcin Kardas, Maria Tsimpoukelli, Mathew Oldham, Mathieu Rita, Maya Pavlova, Melanie Kambadur, Mike Lewis, Min Si, Mitesh Kumar Singh, Mona Hassan, Naman Goyal, Narjes Torabi, Nikolay Bashlykov, Nikolay Bogoychev, Niladri Chatterji, Ning Zhang, Olivier Duchenne, Onur Çelebi, Patrick Alrassy, Pengchuan Zhang, Pengwei Li, Petar Vasic, Peter Weng, Prajwal Bhargava, Pratik Dubal, Praveen Krishnan, Punit Singh Koura, Puxin Xu, Qing He, Qingxiao Dong, Ragavan Srinivasan, Raj Ganapathy, Ramon Calderer, Ricardo Silveira Cabral, Robert Stojnic, Roberta Raileanu, Rohan Maheswari, Rohit Girdhar, Rohit Patel, Romain Sauvestre, Ronnie Polidoro, Roshan Sumbaly, Ross Taylor, Ruan Silva, Rui Hou, Rui Wang, Saghar Hosseini, Sahana Chennabasappa, Sanjay Singh, Sean Bell, Seohyun Sonia Kim, Sergey Edunov, Shaoliang Nie, Sharan Narang, Sharath Raparth, Sheng Shen, Shengye Wan, Shruti Bhosale, Shun Zhang, Simon Vandenhende, Soumya Batra, Spencer Whitman, Sten Sootla, Stephane Collot, Suchin Gururangan, Sydney Borodinsky, Tamar Herman, Tara Fowler, Tarek Sheasha, Thomas Georgiou, Thomas Scialom, Tobias Speckbacher, Todor Mihaylov, Tong Xiao, Ujjwal Karn, Vedanuj Goswami, Vibhor Gupta, Vignesh Ramanathan, Viktor Kerkez, Vincent Gonguet, Virginie Do, Vish Vogeti, Vítor Albiero, Vladan Petrovic, Weiwei Chu, Wenhan Xiong, Wenyin Fu, Whitney Meers, Xavier Martinet, Xiaodong Wang, Xiaofang Wang, Xiaoqing Ellen Tan, Xide Xia, Xinfeng Xie, Xuchao Jia, Xuewei Wang, Yaelle Goldschlag, Yashesh Gaur, Yasmine Babaei, Yi Wen, Yiwen Song, Yuchen Zhang, Yue Li, Yuning

Mao, Zacharie Delpierre Coudert, Zheng Yan, Zhengxing Chen, Zoe Papakipos, Aaditya Singh, Aayushi Srivastava, Abha Jain, Adam Kelsey, Adam Shajnfeld, Adithya Gangidi, Adolfo Victoria, Ahuva Goldstand, Ajay Menon, Ajay Sharma, Alex Boesenberg, Alexei Baevski, Allie Feinstein, Amanda Kallet, Amit Sangani, Amos Teo, Anam Yunus, Andrei Lupu, Andres Alvarado, Andrew Caples, Andrew Gu, Andrew Ho, Andrew Poulton, Andrew Ryan, Ankit Ramchandani, Annie Dong, Annie Franco, Anuj Goyal, Aparajita Saraf, Arkabandhu Chowdhury, Ashley Gabriel, Ashwin Bharambe, Assaf Eisenman, Azadeh Yazdan, Beau James, Ben Maurer, Benjamin Leonhardi, Bernie Huang, Beth Loyd, Beto De Paola, Bhargavi Paranjape, Bing Liu, Bo Wu, Boyu Ni, Braden Hancock, Bram Wasti, Brandon Spence, Brani Stojkovic, Brian Gamido, Britt Montalvo, Carl Parker, Carly Burton, Catalina Mejia, Ce Liu, Changhan Wang, Changkyu Kim, Chao Zhou, Chester Hu, Ching-Hsiang Chu, Chris Cai, Chris Tindal, Christoph Feichtenhofer, Cynthia Gao, Damon Civin, Dana Beaty, Daniel Kreymer, Daniel Li, David Adkins, David Xu, Davide Testuggine, Delia David, Devi Parikh, Diana Liskovich, Didem Foss, Dingkang Wang, Duc Le, Dustin Holland, Edward Dowling, Eissa Jamil, Elaine Montgomery, Eleonora Presani, Emily Hahn, Emily Wood, Eric-Tuan Le, Erik Brinkman, Esteban Arcaute, Evan Dunbar, Evan Smothers, Fei Sun, Felix Kreuk, Feng Tian, Filippos Kokkinos, Firat Ozgenel, Francesco Caggioni, Frank Kanayet, Frank Seide, Gabriela Medina Florez, Gabriella Schwarz, Gada Badeer, Georgia Swee, Gil Halpern, Grant Herman, Grigory Sizov, Guangyi, Zhang, Guna Lakshminarayanan, Hakan Inan, Hamid Shojanazeri, Han Zou, Hannah Wang, Hanwen Zha, Haroun Habeeb, Harrison Rudolph, Helen Suk, Henry Asperegn, Hunter Goldman, Hongyuan Zhan, Ibrahim Damlaj, Igor Molybog, Igor Tufanov, Ilias Leontiadis, Irina-Elena Veliche, Itai Gat, Jake Weissman, James Geboski, James Kohli, Janice Lam, Japhet Asher, Jean-Baptiste Gaya, Jeff Marcus, Jeff Tang, Jennifer Chan, Jenny Zhen, Jeremy Reizenstein, Jeremy Teboul, Jessica Zhong, Jian Jin, Jingyi Yang, Joe Cummings, Jon Carvill, Jon Shepard, Jonathan McPhie, Jonathan Torres, Josh Ginsburg, Junjie Wang, Kai Wu, Kam Hou U, Karan Saxena, Kartikay Khandelwal, Katayoun Zand, Kathy Matosich, Kaushik Veeraraghavan, Kelly Michelena, Keqian Li, Kiran Jagadeesh, Kun Huang, Kunal Chawla, Kyle Huang, Lailin Chen, Lakshya Garg, Lavender A, Leandro Silva, Lee Bell, Lei Zhang, Liangpeng Guo, Licheng Yu, Liron Moshkovich, Luca Wehrstedt, Madian Khabsa, Manav Avalani, Manish Bhatt, Martynas Mankus, Matan Hasson, Matthew Lennie, Matthias Reso, Maxim Groshev, Maxim Naumov, Maya Lathi, Meghan Keneally, Miao Liu, Michael L. Seltzer, Michal Valko, Michelle Restrepo, Mihir Patel, Mik Vyatskov, Mikayel Samvelyan, Mike Clark, Mike Macey, Mike Wang, Miquel Jubert Hermoso, Mo Metanat, Mohammad Rastegari, Munish Bansal, Nandhini Santhanam, Natascha Parks, Natasha White, Navyata Bawa, Nayan Singhal, Nick Egebo, Nicolas Usunier, Nikhil Mehta, Nikolay Pavlovich Laptev, Ning Dong, Norman Cheng, Oleg Chernoguz, Olivia Hart, Omkar Salpekar, Ozlem Kalinli, Parkin Kent, Parth Parekh, Paul Saab, Pavan Balaji, Pedro Rittner, Philip Bontrager, Pierre Roux, Piotr Dollar, Polina Zvyagina, Prashant Ratanchandani, Pritish Yuvraj, Qian Liang, Rachad Alao, Rachel Rodriguez, Rafi Ayub, Raghotham Murthy, Raghu Nayani, Rahul Mitra, Rangaprabhu Parthasarathy, Raymond Li, Rebekkah Hogan, Robin Battey, Rocky Wang, Russ Howes, Ruty Rinott, Sachin Mehta, Sachin Siby, Sai Jayesh Bondu, Samyak Datta, Sara Chugh, Sara Hunt, Sargun Dhillon, Sasha Sidorov, Satadru Pan, Saurabh Mahajan, Saurabh Verma, Seiji Yamamoto, Sharadh Ramaswamy, Shaun Lindsay, Shaun Lindsay, Sheng Feng, Shenghao Lin, Shengxin Cindy Zha, Shishir Patil, Shiva Shankar, Shuqiang Zhang, Shuqiang Zhang, Sinong Wang, Sneha Agarwal, Soji Sajuyigbe, Soumith Chintala, Stephanie Max, Stephen Chen, Steve Kehoe, Steve Satterfield, Sudarshan Govindaprasad, Sumit Gupta, Summer Deng, Sungmin Cho, Sunny Virk, Suraj Subramanian, Sy Choudhury, Sydney Goldman, Tal Remez, Tamar Glaser, Tamara Best, Thilo Koehler, Thomas Robinson, Tianhe Li, Tianjun Zhang, Tim Matthews, Timothy Chou, Tzook Shaked, Varun Vontimitta, Victoria Ajayi, Victoria Montanez, Vijai Mohan, Vinay Satish Kumar, Vishal Mangla, Vlad Ionescu, Vlad Poenaru, Vlad Tiberiu Mihalescu, Vladimir Ivanov, Wei Li, Wencheng Wang, Wenwen Jiang, Wes Bouaziz, Will Constable, Xiaocheng Tang, Xiaojian Wu, Xiaolan Wang, Xilun Wu, Xinbo Gao, Yaniv Kleinman, Yanjun Chen, Ye Hu, Ye Jia, Ye Qi, Yenda Li, Yilin Zhang, Ying Zhang, Yossi Adi, Youngjin Nam, Yu, Wang, Yu Zhao, Yuchen Hao, Yundi Qian, Yunlu Li, Yuzi He, Zach Rait, Zachary DeVito, Zef Rosnbrick, Zhao-duo Wen, Zhenyu Yang, Zhiwei Zhao, and Zhiyu Ma. The llama 3 herd of models, 2024. URL <https://arxiv.org/abs/2407.21783>.

David Ha, Andrew M. Dai, and Quoc V. Le. Hypernetworks. In *International Conference on Learning Representations*, 2017. URL <https://openreview.net/forum?id=rkpACellx>.

Junxian He, Chunting Zhou, Xuezhe Ma, Taylor Berg-Kirkpatrick, and Graham Neubig. Towards a unified view of parameter-efficient transfer learning. In *International Conference on Learning Representations*, 2022. URL <https://openreview.net/forum?id=0RDcd5Axok>.

Dan Hendrycks, Collin Burns, Steven Basart, Andy Zou, Mantas Mazeika, Dawn Song, and Jacob Steinhardt. Measuring massive multitask language understanding. In *ICLR*, 2021. URL <https://arxiv.org/abs/2009.03300>.

Giwon Hong, Emile Van Krieken, Edoardo Ponti, Nikolay Malkin, and Pasquale Minervini. Mixtures of in-context learners. In Wanxiang Che, Joyce Nabende, Ekaterina Shutova, and Mhammad Taher Pilehvar (eds.), *Proceedings of the 63rd Annual Meeting of the Association for Computational Linguistics (Volume 1: Long Papers)*, pp. 26332–26351, Vienna, Austria, July 2025. Association for Computational Linguistics. ISBN 979-8-89176-251-0. doi: 10.18653/v1/2025.acl-long.1277. URL <https://aclanthology.org/2025.acl-long.1277>.

Neil Houlsby, Andrei Giurgiu, Stanislaw Jastrzebski, Bruna Morrone, Quentin De Laroussilhe, Andrea Gesmundo, Mona Attariyan, and Sylvain Gelly. Parameter-efficient transfer learning for NLP. In Kamalika Chaudhuri and Ruslan Salakhutdinov (eds.), *Proceedings of the 36th International Conference on Machine Learning*, volume 97 of *Proceedings of Machine Learning Research*, pp. 2790–2799. PMLR, 09–15 Jun 2019. URL <https://proceedings.mlr.press/v97/houlsby19a.html>.

Edward J Hu, Yelong Shen, Phillip Wallis, Zeyuan Allen-Zhu, Yuanzhi Li, Shean Wang, Lu Wang, and Weizhu Chen. LoRA: Low-rank adaptation of large language models. In *International Conference on Learning Representations*, 2022. URL <https://openreview.net/forum?id=nZeVKeFYf9>.

Gabriel Ilharco, Marco Túlio Ribeiro, Mitchell Wortsman, Ludwig Schmidt, Hannaneh Hajishirzi, and Ali Farhadi. Editing models with task arithmetic. In *The Eleventh International Conference on Learning Representations*, 2023. URL <https://openreview.net/forum?id=6t0Kwf8-jrj>.

Alon Jacovi and Yoav Goldberg. Towards faithfully interpretable NLP systems: How should we define and evaluate faithfulness? In Dan Jurafsky, Joyce Chai, Natalie Schluter, and Joel Tetreault (eds.), *Proceedings of the 58th Annual Meeting of the Association for Computational Linguistics*, pp. 4198–4205, Online, July 2020. Association for Computational Linguistics. doi: 10.18653/v1/2020.acl-main.386. URL <https://aclanthology.org/2020.acl-main.386>.

Josip Jukić and Jan Šnajder. Disentangling latent shifts of in-context learning with weak supervision. In *The Thirty-ninth Annual Conference on Neural Information Processing Systems*, 2025. URL <https://openreview.net/forum?id=tAq9Gxdhr0>.

Andrew Lampinen, Ishita Dasgupta, Stephanie Chan, Kory Mathewson, Mh Tessler, Antonia Creswell, James McClelland, Jane Wang, and Felix Hill. Can language models learn from explanations in context? In Yoav Goldberg, Zornitsa Kozareva, and Yue Zhang (eds.), *Findings of the Association for Computational Linguistics: EMNLP 2022*, pp. 537–563, Abu Dhabi, United Arab Emirates, December 2022. Association for Computational Linguistics. doi: 10.18653/v1/2022.findings-emnlp.38. URL <https://aclanthology.org/2022.findings-emnlp.38>.

Hunter Lang, David Sontag, and Aravindan Vijayaraghavan. Theoretical analysis of weak-to-strong generalization. In *The Thirty-eighth Annual Conference on Neural Information Processing Systems*, 2024. URL <https://openreview.net/forum?id=HOSH0SKk1E>.

Brian Lester, Rami Al-Rfou, and Noah Constant. The power of scale for parameter-efficient prompt tuning. In Marie-Francine Moens, Xuanjing Huang, Lucia Specia, and Scott Wentau Yih (eds.), *Proceedings of the 2021 Conference on Empirical Methods in Natural Language Processing*, pp. 3045–3059, Online and Punta Cana, Dominican Republic, November 2021. Association for Computational Linguistics. doi: 10.18653/v1/2021.emnlp-main.243. URL <https://aclanthology.org/2021.emnlp-main.243>.

Patrick Lewis, Ethan Perez, Aleksandra Piktus, Fabio Petroni, Vladimir Karpukhin, Naman Goyal, Heinrich Köttler, Mike Lewis, Wen-tau Yih, Tim Rocktäschel, Sebastian Riedel, and Douwe Kiela. Retrieval-augmented generation for knowledge-intensive nlp tasks. In H. Larochelle, M. Ranzato, R. Hadsell, M.F. Balcan, and H. Lin (eds.), *Advances in Neural Information Processing Systems*, volume 33, pp. 9459–9474. Curran Associates, Inc., 2020. URL https://proceedings.neurips.cc/paper_files/paper/2020/file/6b493230205f780e1bc26945df7481e5-Paper.pdf.

Xiang Lisa Li and Percy Liang. Prefix-tuning: Optimizing continuous prompts for generation. In Chengqing Zong, Fei Xia, Wenjie Li, and Roberto Navigli (eds.), *Proceedings of the 59th Annual Meeting of the Association for Computational Linguistics and the 11th International Joint Conference on Natural Language Processing (Volume 1: Long Papers)*, pp. 4582–4597, Online, August 2021. Association for Computational Linguistics. doi: 10.18653/v1/2021.acl-long.353. URL <https://aclanthology.org/2021.acl-long.353/>.

Nelson F. Liu, Kevin Lin, John Hewitt, Ashwin Paranjape, Michele Bevilacqua, Fabio Petroni, and Percy Liang. Lost in the middle: How language models use long contexts. *Transactions of the Association for Computational Linguistics*, 12:157–173, 2024. doi: 10.1162/tacl_a_00638. URL <https://aclanthology.org/2024.tacl-1.9/>.

Rabeeh Karimi Mahabadi, James Henderson, and Sebastian Ruder. Compacter: Efficient low-rank hypercomplex adapter layers. In A. Beygelzimer, Y. Dauphin, P. Liang, and J. Wortman Vaughan (eds.), *Advances in Neural Information Processing Systems*, 2021. URL <https://openreview.net/forum?id=bqGK5PyI6-N>.

Sewon Min, Xinxi Lyu, Ari Holtzman, Mikel Artetxe, Mike Lewis, Hannaneh Hajishirzi, and Luke Zettlemoyer. Rethinking the role of demonstrations: What makes in-context learning work? In Yoav Goldberg, Zornitsa Kozareva, and Yue Zhang (eds.), *Proceedings of the 2022 Conference on Empirical Methods in Natural Language Processing*, pp. 11048–11064, Abu Dhabi, United Arab Emirates, December 2022. Association for Computational Linguistics. doi: 10.18653/v1/2022.emnlp-main.759. URL <https://aclanthology.org/2022.emnlp-main.759/>.

Long Ouyang, Jeffrey Wu, Xu Jiang, Diogo Almeida, Carroll Wainwright, Pamela Mishkin, Chong Zhang, Sandhini Agarwal, Katarina Slama, Alex Gray, John Schulman, Jacob Hilton, Fraser Kelton, Luke Miller, Maddie Simens, Amanda Askell, Peter Welinder, Paul Christiano, Jan Leike, and Ryan Lowe. Training language models to follow instructions with human feedback. In Alice H. Oh, Alekh Agarwal, Danielle Belgrave, and Kyunghyun Cho (eds.), *Advances in Neural Information Processing Systems*, 2022. URL <https://openreview.net/forum?id=TG8KACxEON>.

Jonas Pfeiffer, Ivan Vulić, Iryna Gurevych, and Sebastian Ruder. MAD-X: An Adapter-Based Framework for Multi-Task Cross-Lingual Transfer. In Bonnie Webber, Trevor Cohn, Yulan He, and Yang Liu (eds.), *Proceedings of the 2020 Conference on Empirical Methods in Natural Language Processing (EMNLP)*, pp. 7654–7673, Online, November 2020. Association for Computational Linguistics. doi: 10.18653/v1/2020.emnlp-main.617. URL <https://aclanthology.org/2020.emnlp-main.617/>.

Jonas Pfeiffer, Aishwarya Kamath, Andreas Rücklé, Kyunghyun Cho, and Iryna Gurevych. Adapter-Fusion: Non-destructive task composition for transfer learning. In Paola Merlo, Jorg Tiedemann, and Reut Tsarfaty (eds.), *Proceedings of the 16th Conference of the European Chapter of the Association for Computational Linguistics: Main Volume*, pp. 487–503, Online, April 2021. Association for Computational Linguistics. doi: 10.18653/v1/2021.eacl-main.39. URL <https://aclanthology.org/2021.eacl-main.39/>.

Jonas Pfeiffer, Sebastian Ruder, Ivan Vulić, and Edoardo Ponti. Modular deep learning. *Transactions on Machine Learning Research*, 2023. ISSN 2835-8856. URL <https://openreview.net/forum?id=z9EkXfvxta>.

Colin Raffel, Noam Shazeer, Adam Roberts, Katherine Lee, Sharan Narang, Michael Matena, Yanqi Zhou, Wei Li, and Peter J. Liu. Exploring the limits of transfer learning with a unified text-to-text transformer. *Journal of Machine Learning Research*, 21(140):1–67, 2020. URL <http://jmlr.org/papers/v21/20-074.html>.

Nils Reimers and Iryna Gurevych. Sentence-BERT: Sentence embeddings using Siamese BERT-networks. In Kentaro Inui, Jing Jiang, Vincent Ng, and Xiaojun Wan (eds.), *Proceedings of the 2019 Conference on Empirical Methods in Natural Language Processing and the 9th International Joint Conference on Natural Language Processing (EMNLP-IJCNLP)*, pp. 3982–3992, Hong Kong, China, November 2019. Association for Computational Linguistics. doi: 10.18653/v1/D19-1410. URL <https://aclanthology.org/D19-1410/>.

Timo Schick and Hinrich Schütze. Exploiting cloze-questions for few-shot text classification and natural language inference. In Paola Merlo, Jörg Tiedemann, and Reut Tsarfaty (eds.), *Proceedings of the 16th Conference of the European Chapter of the Association for Computational Linguistics: Main Volume*, pp. 255–269, Online, April 2021. Association for Computational Linguistics. doi: 10.18653/v1/2021.eacl-main.20. URL <https://aclanthology.org/2021.eacl-main.20/>.

Miles Turpin, Julian Michael, Ethan Perez, and Samuel R. Bowman. Language models don’t always say what they think: Unfaithful explanations in chain-of-thought prompting. In *Thirty-seventh Conference on Neural Information Processing Systems*, 2023. URL <https://openreview.net/forum?id=bzs4uPLXvi>.

Mitchell Wortsman, Gabriel Ilharco, Samir Ya Gadre, Rebecca Roelofs, Raphael Gontijo-Lopes, Ari S Morcos, Hongseok Namkoong, Ali Farhadi, Yair Carmon, Simon Kornblith, and Ludwig Schmidt. Model soups: Averaging weights of multiple fine-tuned models improves accuracy without increasing inference time. In Kamalika Chaudhuri, Stefanie Jegelka, Le Song, Csaba Szepesvari, Gang Niu, and Sivan Sabato (eds.), *Proceedings of the 39th International Conference on Machine Learning*, volume 162 of *Proceedings of Machine Learning Research*, pp. 23965–23998. PMLR, 17–23 Jul 2022. URL <https://proceedings.mlr.press/v162/wortsman22a.html>.

Sang Michael Xie, Aditi Raghunathan, Percy Liang, and Tengyu Ma. An explanation of in-context learning as implicit bayesian inference. In *International Conference on Learning Representations*, 2022. URL <https://openreview.net/forum?id=RdJVFCHjUMI>.

An Yang, Baosong Yang, Beichen Zhang, Binyuan Hui, Bo Zheng, Bowen Yu, Chengyuan Li, Dayiheng Liu, Fei Huang, Haoran Wei, Huan Lin, Jian Yang, Jianhong Tu, Jianwei Zhang, Jianxin Yang, Jiaxi Yang, Jingren Zhou, Junyang Lin, Kai Dang, Keming Lu, Keqin Bao, Kexin Yang, Le Yu, Mei Li, Mingfeng Xue, Pei Zhang, Qin Zhu, Rui Men, Runji Lin, Tianhao Li, Tianyi Tang, Tingyu Xia, Xingzhang Ren, Xuancheng Ren, Yang Fan, Yang Su, Yichang Zhang, Yu Wan, Yuqiong Liu, Zeyu Cui, Zhenru Zhang, and Zihan Qiu. Qwen2.5 technical report, 2025. URL <https://arxiv.org/abs/2412.15115>.

Zhilin Yang, Peng Qi, Saizheng Zhang, Yoshua Bengio, William Cohen, Ruslan Salakhutdinov, and Christopher D. Manning. HotpotQA: A dataset for diverse, explainable multi-hop question answering. In Ellen Riloff, David Chiang, Julia Hockenmaier, and Jun’ichi Tsujii (eds.), *Proceedings of the 2018 Conference on Empirical Methods in Natural Language Processing*, pp. 2369–2380, Brussels, Belgium, October–November 2018. Association for Computational Linguistics. doi: 10.18653/v1/D18-1259. URL <https://aclanthology.org/D18-1259/>.

A COMPOSITIONALITY BOUND

A.1 PROOF OF THEOREM 1

Let $\phi_1 = G(\mathbf{c}_1)$, $\phi_2 = G(\mathbf{c}_2)$, and $\phi_{12} = G([\mathbf{c}_1; \mathbf{c}_2])$. We aim to bound

$$\|\mathbf{f}_S^{\phi_1+\phi_2}(\mathbf{q}) - \mathbf{f}_T([\mathbf{c}_1; \mathbf{c}_2; \mathbf{q}])\|_2.$$

The Euclidean space $(\mathbb{R}^{|V|}, \|\cdot\|_2)$ satisfies the triangle inequality: for any $a, b, c \in \mathbb{R}^{|V|}$,

$$\|a - c\|_2 \leq \|a - b\|_2 + \|b - c\|_2, \quad (5)$$

where we also use absolute homogeneity (symmetry) of the norm, i.e., $\|b - c\|_2 = \|c - b\|_2$ since $\|-v\|_2 = \|v\|_2$. Apply (5) with

$$a = \mathbf{f}_S^{\phi_1+\phi_2}(\mathbf{q}), \quad b = \mathbf{f}_S^{\phi_{12}}(\mathbf{q}), \quad c = \mathbf{f}_T([\mathbf{c}_1; \mathbf{c}_2; \mathbf{q}]),$$

to obtain

$$\begin{aligned} & \|\mathbf{f}_S^{\phi_1+\phi_2}(\mathbf{q}) - \mathbf{f}_T([\mathbf{c}_1; \mathbf{c}_2; \mathbf{q}])\|_2 \\ & \leq \underbrace{\|\mathbf{f}_S^{\phi_1+\phi_2}(\mathbf{q}) - \mathbf{f}_S^{\phi_{12}}(\mathbf{q})\|_2}_{\text{Term (I)}} + \underbrace{\|\mathbf{f}_S^{\phi_{12}}(\mathbf{q}) - \mathbf{f}_T([\mathbf{c}_1; \mathbf{c}_2; \mathbf{q}])\|_2}_{\text{Term (II)}}. \end{aligned} \quad (6)$$

By parameter sensitivity (3) and generator additivity error (2),

$$\text{Term (I)} \leq L \|\phi_1 + \phi_2 - \phi_{12}\|_2 = L\eta. \quad (7)$$

Apply the student–teacher error (1) to the concatenated context $[\mathbf{c}_1; \mathbf{c}_2]$:

$$\text{Term (II)} \leq \epsilon([\mathbf{c}_1; \mathbf{c}_2]). \quad (8)$$

Combining (6), (7), and (8) yields

$$\|\mathbf{f}_S^{\phi_1+\phi_2}(\mathbf{q}) - \mathbf{f}_T([\mathbf{c}_1; \mathbf{c}_2; \mathbf{q}])\|_2 \leq L\eta + \epsilon([\mathbf{c}_1; \mathbf{c}_2]),$$

which proves Theorem 1. \square

Corollary 1 (Extension to k contexts). *By induction, Theorem 1 extends to any sequence of contexts $\mathbf{c}_1, \dots, \mathbf{c}_k$ with corresponding adapters $\phi_i = G(\mathbf{c}_i)$:*

$$\|\mathbf{f}_S^{\sum_{i=1}^k \phi_i}(\mathbf{q}) - \mathbf{f}_T([\mathbf{c}_1; \dots; \mathbf{c}_k; \mathbf{q}])\|_2 \leq (k-1)L\eta + \epsilon([\mathbf{c}_1; \dots; \mathbf{c}_k]).$$

A.2 GEOMETRIC INTERPRETATION

Adapters $\phi = G(\mathbf{c})$ can be viewed as vectors in the parameter space Φ . In the ideal case, G embeds contexts into a flat subspace where concatenation in input space corresponds exactly to vector addition in parameter space. The deviation terms then acquire a geometric meaning: η measures the generator’s departure from additivity, and $\epsilon([\mathbf{c}_1; \mathbf{c}_2])$ captures the student’s misalignment with the teacher on concatenated contexts. The Lipschitz constant L governs how deviations in adapter space propagate into the model’s output space. Compositionality can therefore be understood as flattening the contextual geometry into a nearly linear embedding, with small η and ϵ ensuring that adapter addition faithfully mirrors context concatenation.

B EXPERIMENTAL SETUP AND HYPERPARAMETERS

B.1 DATA

For MMLU (Hendrycks et al., 2021), which comprises 59 subject-specific subsets, we report accuracy averaged across all subsets. We train a *single generator* jointly across all subsets. This ensures that the generator is shared across domains rather than tuned separately per subject. For weak supervision during generator optimization, we sample queries and contexts from the validation split

Table 5: Parameter counts for base models and our framework. Student parameters correspond to LoRA adapters attached to the base LM, while generator parameters denote the generator network itself. Generator adapter counts indicate the size of parameters produced per context. Total trainable parameters are the sum of student and generator parameters.

Model	Base LLM	Student adapter	Generator adapter	Generator (total)
Llama 3.1 (8B)	8.03B	21M	42M	210M
Llama 3.2 (3B)	3.19B	4.2M	8.4M	42M
Qwen 2.5 (7.6B)	7.61B	20M	40M	180M

without using ground-truth labels, while demonstrations are drawn (with labels) from the training split. Evaluation is performed on the held-out test split.

For ARC-Challenge (Clark et al., 2018), we follow the same setup: unlabeled validation examples provide queries and contexts for weak supervision, labeled demonstrations are drawn from the training set, and performance is reported on the test set.

For HotpotQA (Yang et al., 2018), we restrict context inputs to the relevant gold supporting passages associated with each question. We sample 10k examples stratified across difficulty levels, and partition them into 5k for training, 3k for validation, and 2k for testing.

B.2 MODELS

We summarize the main characteristics of the base LMs used in our experiments in Table 5, together with the sizes of the student and generator adapters. We use the `bfloat16` half-precision format for all model parameters.

B.3 METHODS

For GenAda (Chen et al., 2025) and WILDA (Jukić & Šnajder, 2025), we use the default hyperparameters and follow the training procedures described in the respective papers. To ensure comparability, we adopt an identical configuration for adapter sizes and target modules across all methods; these design choices are detailed in the following section.

B.4 HYPERPARAMETERS

Optimization. For each dataset and model combination, we train the generator parameters with AdamW (weight decay 0.01) for 10 epochs. The learning rate is set to 10^{-4} with 5% linear warmup followed by cosine decay.

Loss weights. We set $\lambda_{ST} = 1.0$, $\lambda_{ADD} = 0.5$, and $\lambda_{RECON} = 0.1$. These values balance (i) fidelity to teacher logits through student–teacher alignment, (ii) enforcement of compositionality via additivity regularization, and (iii) auxiliary reconstruction for stability and faithfulness, while avoiding over-regularization.

Adapter configuration. We insert LoRA adapters into all attention projections (q , k , v , and o) as well as into the MLP down- and up-projection layers. For the generator, we use a uniform rank of 32 across all modules, while for the student we use rank 16. Following standard practice, each LoRA module applies a scaling factor α , such that the effective weight update is $\frac{\alpha}{r}AB$. We set $\alpha = 32$ for generator adapters and $\alpha = 16$ for student adapters, ensuring balanced contribution of low-rank updates relative to their respective ranks.

Reconstruction under composition. In the compositional setting, where multiple adapters are generated for different contexts and summed, we compute the reconstruction F1 score in a permutation-invariant fashion. This adjustment is necessary because the generator is explicitly incentivized to be commutative, i.e., $G([c_1; c_2]) \approx G(c_1) + G(c_2) = G(c_2) + G(c_1)$. Concretely, for multiple contexts, we evaluate reconstruction across all possible permutations and report the

Table 6: XSUM summarization with LLaMA-3.1 8B. We report ROUGE-1 (R1), ROUGE-2 (R2), and ROUGE-L (RL) F1. R1 and R2 measure unigram and bigram overlap with the reference summary, while RL measures the longest common subsequence. Higher values indicate closer alignment with the reference and better summary quality.

Method	R1 \uparrow	R2 \uparrow	RL \uparrow
ICL	36.1	15.6	28.4
PBFT	38.3	18.1	31.6
GenAda	33.4	13.1	25.6
COMPAS	41.8	22.8	33.5

score corresponding to the most successful ordering. This ensures that the metric reflects content preservation rather than sensitivity to input order.

Generator variants. In addition to the default *Adapter* generator used in COMPAS, we consider two alternatives for ablation. The *RNN* variant employs a lightweight two-layer gated recurrent unit (GRU; Cho et al., 2014) with hidden size 256 to aggregate token-level context representations before projecting them into a compact latent space, followed by an up-projection to the full set of student adapter parameters. The *Linear* variant removes both the GRU and the generator adapter; instead, the pooled context representation is passed through a single linear bottleneck and then expanded directly into the student adapter parameter space.

B.5 COMPUTING INFRASTRUCTURE

We conducted our experiments on a mix of local and cluster resources. Local training was performed on a workstation with an AMD Ryzen Threadripper 3970X 32-Core CPU, 256GB RAM, and 2× NVIDIA GeForce RTX 3090 GPUs (24GB each). Larger-scale runs were executed on a compute cluster equipped with 2× NVIDIA A100 GPUs (40GB each).

C ADDITIONAL EXPERIMENTS

C.1 LONG-FORM SUMMARIZATION

Beyond question answering, we also evaluate whether the representations learned by COMPAS generalize to long-form generation tasks. Its reconstruction objective already requires producing full demonstrations and multi-paragraph passages (Table 3), exercising long-range generation in training.

To test generalization capabilities beyond QA, we additionally evaluate COMPAS on XSUM, a standard abstractive summarization benchmark. Results are reported in Table 6. COMPAS achieves the strongest performance across all ROUGE metrics, substantially outperforming ICL and other baselines. This indicates that the learned context-to-parameter mapping transfers to tasks that require extended, structured generation, supporting the use of COMPAS as a general parametrization mechanism.

C.2 SUPERVISED AND PROMPT-BASED BASELINES

We further evaluate supervised and parametric baselines: (i) pattern-based fine-tuning (PBFT), optimized with a cloze-style language modeling objective (Schick & Schütze, 2021); (ii) a linear SFT head trained on top of the frozen backbone; (iii) prefix-tuning with the same demonstrations (Li & Liang, 2021); and (iv) an ICL variant that retrieves the top- k most similar demonstrations for each query using SBERT embeddings (Reimers & Gurevych, 2019).

Results for MMLU and ARC are reported in Table 7. Across both benchmarks, COMPAS consistently outperforms all supervised and prompt-based baselines, supporting that its improvements arise from the context-to-parameter mechanism rather than differences in data, supervision, or training procedure.

Table 7: Supervised and prompt-based baselines with LLaMA-3.1 8B. We report mean accuracy on MMLU and ARC over 10 runs with 16 demonstrations in total. COMPAS is evaluated with 4×4 composition. Standard deviations are shown in subscript, and the best results are in bold.

Method	MMLU	ARC
ICL (16-shot)	$64.2_{1.8}$	$74.2_{1.6}$
ICL + prefix-tuning	$66.1_{1.4}$	$74.0_{1.3}$
ICL + similarity selection	$68.1_{0.6}$	$75.5_{0.2}$
PBFT (labels only)	$66.8_{1.1}$	$75.6_{1.0}$
Linear SFT head	$62.1_{1.5}$	$71.3_{1.4}$
COMPAS (4×4)	$72.2_{0.3}$	$81.3_{0.3}$

Table 8: Position-aware reconstruction evaluation. We report positional ROUGE-L F1 for context pair permutations from HotpotQA for the commutative baseline without positional encoding (No-PE) and a simple position-aware variant (PE-Tag), and slot-based positional embeddings (Slot-PE). Scores are mean with standard deviation as subscripts over 10 runs.

	LLaMA-3.1 8B	LLaMA-3.2 3B	Qwen-2.5 7B
No-PE (commutative linear)	$62.5_{2.0}$	$50.1_{2.2}$	$60.4_{2.1}$
Slot-PE	$87.6_{0.9}$	$71.1_{2.6}$	$85.0_{1.4}$

C.3 POSITIONAL ENCODING AND ORDER SENSITIVITY

By design, our generator enforces *commutativity*, i.e., $G([c_1; c_2]) \approx G(c_1) + G(c_2) = G(c_2) + G(c_1)$, which is desirable for tasks where order invariance is beneficial and directly reduces η . The trade-off is that strict commutativity removes the ability to encode order.

As a *proof of concept*, we conduct an experiment on HOTPOTQA using pairs of supporting contexts. We augment the generator with *slot embeddings*, i.e., for slot i we add a learnable vector s_i to the corresponding adapter delta:

$$\tilde{\phi}_i = G(c_i) + s_i, \quad \Phi = \sum_i \tilde{\phi}_i. \quad (9)$$

This introduces positional variance while preserving linear composition, thereby allowing the model to distinguish $[c_1; c_2]$ from $[c_2; c_1]$.

Results in Table 8 suggest that order sensitivity can be layered on top of the commutative backbone when tasks require it, though we leave a systematic study to future work.

C.4 COMPOSITIONAL SCALING

A central design choice in COMPAS is how context is partitioned into blocks prior to adapter generation. Block size controls both how much information is encoded into a single adapter and how many such adapters must be composed at inference time, and therefore directly influences both expressiveness and compositional stability. We next examine how this tradeoff affects accuracy and additivity as the total number of demonstrations increases.

Table 9 shows how block structure affects both task accuracy and compositional fidelity. For a fixed number of demonstrations, COMPAS reaches its best performance with intermediate block sizes (approximately 4–8 demonstrations per block), which yield both higher MMLU accuracy and lower additivity error η .

When blocks become too large (e.g., 2×16 or 1×16), the generator must encode many demonstrations jointly, which weakens the linear structure of the latent parameterization and increases additivity error. Conversely, when blocks become too small (e.g., 16×1), each block provides a limited contextual signal, leading to slightly reduced accuracy and moderately higher η .

As the total number of demonstrations increases, accuracy steadily improves, demonstrating that COMPAS benefits from additional evidence. In practice, the maximum feasible block size is limited

Table 9: Effect of block granularity and scaling on MMLU accuracy and additivity error η with LLaMA 8B. We vary the block structure for a fixed total number of demonstrations and report accuracy and generator additivity error.

Total demos	Method	Accuracy	$\eta \downarrow$
16	ICL (16-shot)	64.2	–
16	COMPAS (4×4)	72.2	0.08
16	COMPAS (2×8)	70.9	0.11
16	COMPAS (1×16)	69.4	0.15
16	COMPAS (16×1)	71.3	0.09
32	ICL (32-shot)	65.5	–
32	COMPAS (8×4)	73.1	0.07
32	COMPAS (4×8)	74.0	0.09
32	COMPAS (2×16)	72.4	0.19
40	COMPAS (5×8)	74.3	0.10
48	COMPAS (6×8)	74.9	0.09
56	COMPAS (7×8)	75.4	0.12
64	COMPAS (8×8)	76.2	0.16

by GPU memory, since larger blocks require the generator to encode more tokens jointly. Within these limits, using moderately sized blocks provides a favorable tradeoff between representation stability and information density.

Finally, long-context ICL baselines can only be evaluated reliably up to 32 demonstrations due to memory constraints. In contrast, COMPAS decouples inference cost from context length, enabling evaluation with more demonstrations on the same hardware through compositional adapter merging.

C.5 ROBUSTNESS TO NOISY CONTEXT

In practical retrieval-based systems, the contexts provided to a model are often imperfect: demonstrations may contain incorrect labels, multiple sources may disagree about the same example, or retrieved passages may be unrelated to the query. We therefore evaluate how COMPAS behaves under controlled perturbations that explicitly simulate these failure modes and compare it directly to standard ICL under identical corruption patterns.

We introduce three types of degradation at inference time. *Noisy demonstrations* are generated by randomly flipping the labels of a fixed fraction of the in-context examples (12.5% and 25% of the 16 demonstrations), while keeping inputs unchanged. This simulates annotation errors or unreliable retrieval from weakly supervised corpora. *Contradictory demonstrations* are constructed by duplicating a subset of examples and assigning them conflicting labels: for 4 of the 16 demonstrations, the same input appears twice across contexts, once with the correct label and once with an incorrect label. This explicitly creates inconsistent supervision inside the context and mimics disagreement between retrieved sources or conflicting knowledge bases. *Off-topic contamination* is introduced by appending unrelated paragraphs sampled from HotpotQA to the end of the context, increasing the number of irrelevant tokens without changing the gold demonstrations. This simulates retrieval failures in which non-informative or spurious documents are mixed into the prompt. All results are reported as averages over 10 independent runs with different random corruption patterns.

Table 10 reports accuracy on MMLU as the demonstration noise increases. Both methods degrade as noise grows, but COMPAS consistently retains a clear performance margin. Notably, the gap widens under stronger label corruption and remains substantial under contradictory supervision. This suggests that compositional context encoding is more robust to internally inconsistent evidence than raw concatenation: while ICL treats all tokens uniformly, COMPAS compresses each demonstration into a latent representation, reducing the impact of spurious or conflicting signals.

Table 11 reports results on HotpotQA as irrelevant passages are injected into the context. ICL performance degrades steadily as more off-topic content is introduced, indicating sensitivity to prompt dilution and distraction effects. In contrast, COMPAS remains comparatively stable and preserves

Table 10: Robustness under noisy and contradictory demonstrations on MMLU with LLaMA 8B (mean over 10 runs).

Method	Clean	12.5% noise	25% noise	Contradictory
ICL	66.5	62.1	58.7	57.9
COMPAS	72.2	71.3	69.4	68.4

Table 11: HotpotQA under off-topic context contamination with LLaMA 8B. Accuracy with irrelevant paragraphs appended to the context (mean over 10 runs).

Method	Clean	+1 off-topic	+2 off-topic
ICL	82.0	79.4	77.6
COMPAS	82.9	82.3	81.7

most of its clean-context accuracy even as irrelevant text grows. This behavior is consistent with the hypothesis that encoding context into parameters rather than raw tokens makes inference less sensitive to unrelated input.

Taken together, these experiments demonstrate that composition-based context parametrization improves robustness to realistic retrieval noise. Even when demonstrations contain errors, contradictions, or irrelevant information, COMPAS degrades more gracefully than ICL, supporting additive composition as a stabilizing mechanism under imperfect and noisy context conditions.

C.6 EFFICIENCY

We compare the computational and memory efficiency of COMPAS to standard ICL prompting using LLaMA 8B on ARC-Challenge. Table 12 reports FLOPs speedup (relative to ICL with the same number of demonstrations k) and peak inference memory. Results are averaged over 10 runs on a sample of 1k test queries. As expected, the memory cost of ICL grows linearly with the number of demonstrations, since the model must re-encode all tokens at inference. In contrast, COMPAS amortizes context encoding into a one-shot parameter generation step, so inference depends only on the query length. This yields substantial speedups that increase with k : 2.2 \times at 4-shot, 3.7 \times at 12-shot, and 4.1 \times at 16-shot. Memory usage shows a similar trend, with ICL increasing steadily as more demonstrations are added, while COMPAS remains nearly constant across different k . This demonstrates that COMPAS not only improves accuracy, but also yields more efficient and scalable inference by decoupling compute and memory from context length.

Additionally, Table 13 compares absolute inference and training compute across methods. The methods differ primarily in their training regimes. WILDA is inexpensive for a single demonstration configuration, but does not amortize: each new context requires a separate fine-tuning run. GenAda incurs a large one-time training cost to learn a generator. COMPAS lies between these extremes, training a generator once at moderate cost and reusing it across contexts. In cumulative terms, WILDA’s total cost grows linearly with the number of demonstration configurations and overtakes COMPAS after approximately 17 contexts, beyond which repeated fine-tuning becomes more expensive than the one-time generator training of COMPAS. At the same time, COMPAS is approximately 13 \times cheaper to train than GenAda, while achieving comparable inference-time efficiency. Thus, COMPAS provides a favorable tradeoff between repeated fine-tuning and large upfront training cost, combining amortization with moderate training overhead.

Table 12: Efficiency comparison of ICL vs. COMPAS with LLaMA 8B. We report speedups in FLOPs for COMPAS inference relative to ICL with k demonstrations, and peak inference memory (GB). Results are averaged over 10 runs on ARC-Challenge. COMPAS replaces long-context prompts with adapters, reducing both compute and memory usage.

Method	Speedup (FLOPs rel. to ICL@k) \uparrow				Peak memory (GB) \downarrow			
	4	8	12	16	4	8	12	16
ICL (prompting)	1.0 \times	1.0 \times	1.0 \times	1.0 \times	22.1	27.3	33.5	37.9
COMPAS	2.2 \times	3.1 \times	3.7 \times	4.1 \times	17.2	17.9	18.1	19.4

Table 13: Absolute compute comparison with LLaMA 8B. We report absolute inference-time compute per query and training compute in TFLOPs on the ARC-Challenge dataset using 16 demonstrations in total with 4×4 composition for COMPAS. WILDA trains a new adapter for each demonstration configuration, whereas GenAda and COMPAS train a generator once and amortize across different contexts.

Method	Inference TFLOPs / query	Training TFLOPs	Regime
ICL (prompting)	4.0	–	No training
WILDA	0.7	1.4×10^5	Per demo set
GenAda	0.9	3.1×10^7	One-time
COMPAS	0.8	2.4×10^6	One-time

D PROMPT TEMPLATES

D.1 TEMPLATES FOR MULTI-CHOICE QUESTION ANSWERING

Generic prompt template MMLU and ARC-Challenge

Demonstrations:

```
Question: {Previous Question 1}
Answer choices:
(A: {Choice A1}),
(B: {Choice B1}),
(C: {Choice C1}),
(D: {Choice D1})
Answer: (Correct Answer 1)
```

```
Question: {Previous Question 2}
Answer choices:
(A: {Choice A2}),
(B: {Choice B2}),
(C: {Choice C2}),
(D: {Choice D2})
Answer: (Correct Answer 2)
...
```

Query:

```
Question: {Current Question}
Answer choices:
(A: {Choice A}),
(B: {Choice B}),
(C: {Choice C}),
(D: {Choice D})
Answer: (
```

D.2 MMLU EXAMPLES

Example for MMLU abstract algebra

Demonstrations:

Question: Find the maximum possible order for an element of S_n for $n = 10$.

Answer choices:

- (A: 6),
- (B: 12),
- (C: 30),
- (D: 105)

Answer: (C: 30)

Question: Compute the product in the given ring. $(2, 3)(3, 5)$ in $\mathbb{Z}_5 \times \mathbb{Z}_9$

Answer choices:

- (A: (1, 1)),
- (B: (3, 1)),
- (C: (1, 6)),
- (D: (3, 6))

Answer: (D: (3, 6))

Query:

Question: If (G, \cdot) is a group such that $(ab)^{-1} = a^{-1}b^{-1}$ for all a, b in G , then G is a/an

Answer choices:

- (A: commutative semigroup),
- (B: abelian group),
- (C: non-abelian group),
- (D: None of these)

Answer: (

D.3 ARC-CHALLENGE EXAMPLES

Example for ARC-Challenge

Demonstrations:

Question: Based on their locations in the periodic table, which element has chemical properties most similar to those of calcium, Ca?

Answer choices:

- (A: beryllium, Be),
- (B: potassium, K),
- (C: titanium, Ti),
- (D: yttrium, Y)

Answer: (A: beryllium, Be)

Question: Which term best describes the life cycle of an insect that reaches the adult stage without being a pupa?

Answer choices:

- (A: incomplete metamorphosis),
- (B: complete metamorphosis),
- (C: alternation of generations),
- (D: spontaneous mutation)

Answer: (A: incomplete metamorphosis)

Query:

Question: Which property of a mineral can be determined

just by looking at it?

Answer choices:

- (A: luster),
- (B: mass),
- (C: weight),
- (D: hardness)

Answer: (

D.4 HOTPOTQA EXAMPLE

Example for HotpotQA

Question:

Who invented the type of script used in autographs?

Supporting Context:

(Cuneiform script):

Cuneiform script, one of the earliest systems of writing, was invented by the Sumerians. It is distinguished by its wedge-shaped marks on clay tablets, made by means of a blunt reed for a stylus. The name "cuneiform" itself simply means "wedge shaped".

(Autograph in Assyriology):

An autograph in Assyriology is the hand-copy of a cuneiform clay-tablet. Producing an autograph is often the first step of a tablet's archaeological interpretation and the autograph is frequently the authoritative form that is published as source material. Autographing the text is followed by transliteration, transcription and translation.

Answer: Sumerians

E LIMITATIONS

Order-insensitivity of composition. In COMPAS, parameter-space composition is strictly commutative and associative, since adapters are summed without regard to order. This differs from textual concatenation, where (c_A, c_B) and (c_B, c_A) may yield different interpretations. While our results show benefits of order-robustness (mitigating prompt-order sensitivity), the lack of positional information may reduce expressivity in tasks where sequence order is essential, such as instruction chaining or narrative reasoning. In additional experiments, we provide a proof of concept showing that positional information can be encoded within the generator, demonstrating feasibility but leaving systematic exploration to future work.

Generator robustness. Our generator is trained on a meta-distribution of contexts and shows cross-domain transfer, but generalization to entirely novel domains or reasoning styles is not guaranteed. In particular, low-resource or highly specialized tasks may expose brittle adaptation.

Linearity vs. expressivity. The framework enforces strict linear compositionality of adapters to ensure interpretability and additivity guarantees. However, some tasks inherently require non-linear interactions between contexts (e.g., resolving contradictions or multi-hop reasoning). In such cases, COMPAS may face a trade-off between maintaining modularity and achieving task-optimal integration.

Scalability and efficiency trade-offs. Although COMPAS replaces long contexts with compact adapters, the generator itself introduces a large up-projection layer whose parameter count grows

with the size of the student adapters. This overhead is modest relative to the base LM but still significant. Scaling to even larger backbones or more complex adapter schemes may therefore incur efficiency and memory costs that partially offset the gains from shorter inference contexts.

LLM USAGE DISCLOSURE

In preparing this manuscript, we used LLMs to polish the writing at the sentence level. This assistance was limited to stylistic improvements such as grammar, clarity, and conciseness.